

# On Kinematic Instability of Parallel Robots

John F. O'Brien and John T. Wen

Center for Automation Technology  
Department of Electrical, Computer, & Systems Engineering  
Rensselaer Polytechnic Institute, Troy, NY 12180  
{obrien,wen}@cat.rpi.edu

## Abstract

Parallel mechanisms frequently contain an unstable type of singularity that has no counterpart in serial mechanisms. When the mechanism is at or near this type of singularity, it loses the ability to counteract external forces in certain directions. The determination of unstable singular configurations in parallel robots is not trivial, and is usually attempted via exhaustive search of the workspace using an accurate analytical model of the mechanism kinematics.

This paper investigates the determination of unstable singular poses for the platform type of parallel mechanisms using a coordinate-independent approach. We also suggest a joint braking method for the trajectory control in the presence of such singularities.

## 1 Introduction

Parallel robots provide a stiff connection between the payload and the base structure, with pose accuracy that is superior to serial chain manipulators. The principal drawbacks concerning parallel robots are their limited workspace, and the complexity of singularity analysis [5, 6, 7]. In contrast to serial chain manipulators, singularities in parallel mechanisms have different manifestations. This issue has been studied in the multi-finger grasping context in [8, 9] and more recently for general parallel mechanisms in [10, 11, 14]. In [10], the singularities are separated into two broad classifications: end-effector and actuator singularities. The former is comparable to the serial arm case, where the end-effector loses a degree-of-freedom in the task space. The latter is defined when a certain task wrench cannot be resisted by active joint torques. Or equivalently, the task frame can move even when all the active joints are locked. These are called the unstable configurations in [14] which correspond to unstable grasps in the multi-finger grasp literature. The unstable type of singularity is obviously unattractive, as unpredictable task motion could result.

The singularity condition in parallel mechanisms has been addressed using manipulability measures. Bicchi et al. [8] present a manipulability measure for multifingered grasps in the form of a Rayleigh Quotient, and presents methods of finding minimum effort trajectories. This work is expanded to include passivity in the joint space in [11, 12]. Gosselin and Angeles [15] start with a modified version of the fundamental grasping constraint where *active* joint rates are mapped to task rates, and defines three types of singularity via the calculation of the determinant of two matrices. This is later used to develop a kinematic isotropy measure implemented as a design tool in [21]. Chiacchio et al. [9] explore the velocity-torque duality and find the composite Jacobian by post-multiplying the hand Jacobian by the psuedoinverse of the grasp map. The paper provides examples of cooperative mechanisms to compare the system level approach to force-velocity polytopes in [22]. Park et al. [10] employs a psuedo-Riemannian metric to analyze manipulability. The method treats passivity in the joint space and mechanism redundancy, and gives an excellent treatment of the non-degenerate and degenerate actuator singularity.

Several authors have proposed methods to determine unstable configurations in platform manipulators through direct analysis of the forward kinematic constraints [1, 2, 3]. In [1], Husty investigates seven constraint equations found from the forward kinematics of the Griffis-Duffy type platform. He shows that the mechanism exhibits self-motion of the end-effector at every pose in its workspace.

Actuator redundancy is proposed to deal with singularities and improve mechanism isotropy in the development of a spherical parallel manipulator in the work by Leguay-Durand and Reboulet [25]. Actuator

redundancy is also used in Ryu et al. [16, 17, 18] to eliminate unstable singularities found after the fabrication of the Eclipse universal machining mechanism.

This paper reviews the differential kinematics of general parallel mechanisms, and addresses the determination of unstable end-effector poses of platform type of parallel mechanisms using a coordinate-independent approach. The paper then addresses trajectory control of such mechanisms by using brakes in the neighborhood of unstable singularities.

*Terminology and Notation:* Given a matrix  $G$ , we use  $\tilde{G}$  to either denote the annihilator of  $G$  ( $\tilde{G}G = 0$ ) or the transpose of the annihilator of  $G^T$  ( $G\tilde{G} = 0$ ). The distinction between the two cases will be clear from the context.

## 2 Differential Kinematics of Parallel Robots

This section considers the differential kinematics of general rigid multibody systems. Consider a general mechanism subject to kinematic constraints. The generalized coordinate (with the constraints removed) is denoted by  $\theta$ . The active joint angles are denoted by  $\theta_a$  and passive ones by  $\theta_p$ . We order the angles so that  $\theta^T = [\theta_a^T, \theta_p^T]$ . For platform type of mechanisms, the kinematics are given by the grasping constraint:

$$J_h \dot{\theta} = G^T v_T \quad (1)$$

The tall matrices  $G^T$  and  $J_h$  (the Grasp Map and hand Jacobian, respectively) map the joint to task body velocities that satisfy the constraints associated with the contacts between individual mechanism fingers and the grasped object. For force closure grasps, (1) can be rewritten.

$$v_T = G^{T\dagger} J_h \dot{\theta} = J_T \dot{\theta} \quad (2)$$

$$0 = \tilde{G}^T J_h \dot{\theta} = J_C \dot{\theta} \quad (3)$$

where  $\tilde{G}^T$  is the annihilator of  $G^T$ . Partition  $J_C$  and  $J_T$  according to the dimension of  $\theta_a$  and  $\theta_p$ :

$$J_C = [ J_{C_a} \quad J_{C_p} ] \quad J_T = [ J_{T_a} \quad J_{T_p} ] .$$

Then (3) can be used to solve for  $\dot{\theta}_p$ :

$$\dot{\theta}_p = -J_{C_p}^\dagger J_{C_a} \dot{\theta}_a + \tilde{J}_{C_p} \xi \quad (4)$$

where  $\text{col}(\tilde{J}_{C_p})$  spans the null space of  $J_{C_p}$ , and  $\xi$  is arbitrary. Substituting into (2), we have

$$v_T = (J_{T_a} - J_{T_p} J_{C_p}^\dagger J_{C_a}) \dot{\theta}_a + J_{T_p} \tilde{J}_{C_p} \xi. \quad (5)$$

Define the composite manipulability Jacobian as

$$\bar{J}_T = J_{T_a} - J_{T_p} J_{C_p}^\dagger J_{C_a}. \quad (6)$$

In this paper, we will not address mechanisms that are under- or redundantly actuated, thus  $\bar{J}_T$  is square. There are two cases of singularities in parallel robots:

1. Unmanipulable Singularity: This corresponds to configurations at which  $\bar{J}_T$  loses rank (minimum singular value of  $\bar{J}_T$  is zero).
2. Unstable Singularity: This corresponds to configurations at which  $J_{T_p} \tilde{J}_{C_p} \neq 0$  (maximum singular value of  $\bar{J}_T$  is infinite).

It may happen that  $J_{T_p} \tilde{J}_{C_p} = 0$  but  $\tilde{J}_{C_p} \neq 0$ . This corresponds to the existence of self motion involving only passive joints in the mechanism but does not affect the task motion.

We can now define the manipulability ellipsoid as the ellipsoid corresponding to  $\bar{J}_T$ . Additional weighting matrices for active joint velocities and task velocities can also be included. Manipulability ellipsoids provide a geometric visualization for singular configurations. At an unmanipulable singularity, the ellipsoid becomes degenerate (the length of one or more axes become zero, implying that the ellipsoid has zero volume).

At an unstable singularity, the ellipsoid becomes infinite (the length of one or more axes become infinite, implying that arbitrary task velocity is possible even when active joint velocities are constrained). When the mechanism is at a configuration close to an unstable singularity, the ellipsoid would become badly conditioned as one or more axes would be very large. When the mechanism is close to an unmanipulable configuration, the ellipsoid would also be badly conditioned, since the length of one or more of the axes will be close to zero. Hence, a measure of the “closeness” to singularity may be chosen to be the condition number of  $\bar{J}_T$ . However, this measure should be used in conjunction with the minimum singular value of  $\bar{J}_T$  to distinguish between the two types of singularities.

The unstable singularity, unique to parallel mechanisms, presents a dangerous situation. When the mechanism moves through these poses, it is unable to resist specific task wrenches, which can result in undesirable and unavoidable end-effector motions.

## 2.1 Unstable Singularity in Platform Type Parallel Mechanisms: A Closer Look

Finding solutions to  $0 = \frac{1}{\det(\bar{J}_T)}$  is difficult, thus determination of unstable configurations in parallel mechanisms is usually performed by an exhaustive search of the workspace using an accurate inverse kinematic model. This is not only computationally intensive, especially for 6-DOF mechanisms, but also is not guaranteed to discover these poses [16].

In this section, we take a coordinate independent approach to finding the singularities. The 6-DOF Eclipse [16] will be used to illustrate the approach. We will focus on representing  $J_{C_p}$  in a coordinate-independent form.

Consider the 6-DOF parallel mechanism shown in Figures 1–2. The origin of the inertial frame,  $O$ , is chosen to be at the center of the base. The three base joints, denoted  $a, b, c$ , rotate about  $O$ . Each base joint is connected to a prismatic joint which in turn connects to a 1-DOF revolute joint with the axis of rotation tangential to the base circle. The three revolute joints, denoted  $1, \dots, 3$ , connect to corresponding spherical joints, denoted  $4, \dots, 6$ , spaced symmetrically about the platform.

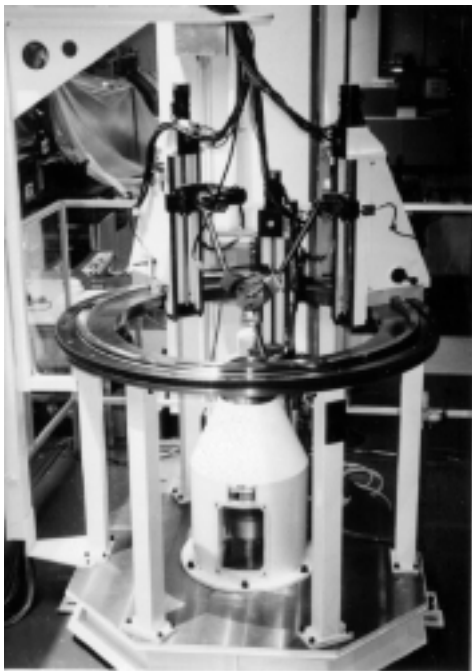


Figure 1: Picture of Eclipse (used with permission from the Seoul National University)

The forward kinematics can be compactly written in the following form:

$$R_{0E} = R_{01}R_{14}R_{4E}$$

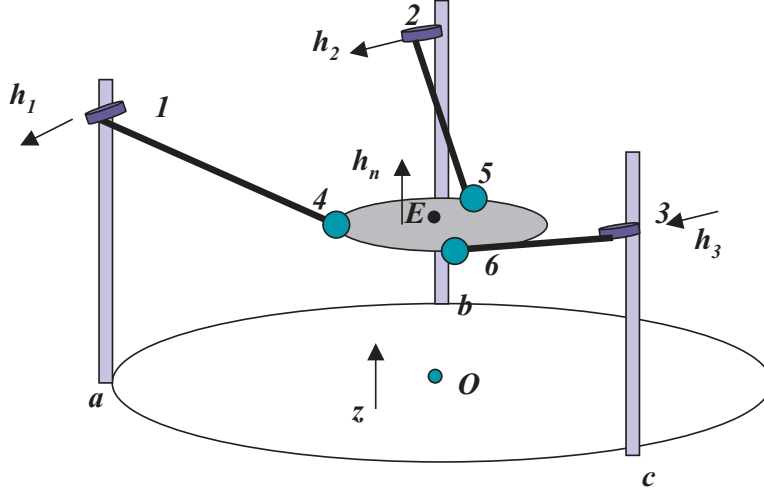


Figure 2: Schematics of Eclipse

$$\begin{aligned}
 &= R_{02}R_{25}R_{5E} \\
 &= R_{03}R_{36}R_{6E}
 \end{aligned} \tag{7}$$

$$\begin{aligned}
 \vec{p}_{0E} &= \vec{p}_{0a} + \vec{p}_{a1} + \vec{p}_{14} + \vec{p}_{4E} \\
 &= \vec{p}_{0b} + \vec{p}_{b2} + \vec{p}_{25} + \vec{p}_{5E} \\
 &= \vec{p}_{0c} + \vec{p}_{c3} + \vec{p}_{36} + \vec{p}_{6E}
 \end{aligned} \tag{8}$$

Let  $\hat{v}$  denote the cross product form of the vector  $v$ ,  $\theta_{0i}$  the rotation angles of the base joints, and  $\theta_{i,i+3}$  the rotation angles of the pivot joints, we have

$$R_{0i} = e^{\hat{z}\theta_{0i}} \quad R_{i,i+3} = e^{\widehat{R_{0i}h_i}\theta_{i,i+3}}$$

where  $z = [0 \ 0 \ 1]^T$ ,  $h_i$  is the tangent vector to the base circle at the base joint, written in the inertial frame, when the mechanism is in the zero configuration. Written in the inertial frame, the translational kinematics is

$$\begin{aligned}
 p_{0E} &= R_{01}p_{0a} + R_{01}zd_1 + R_{01}R_{14}p_{14} + R_{0E}p_{4E} \\
 &= R_{02}p_{0b} + R_{02}zd_2 + R_{02}R_{25}p_{25} + R_{0E}p_{5E} \\
 &= R_{03}p_{0c} + R_{03}zd_3 + R_{03}R_{36}p_{36} + R_{0E}p_{6E}.
 \end{aligned}$$

Note that we have parameterized the prismatic joint so that the length of the joint is 0 at the zero configuration.

The three base revolute joints (rotation about the base circle) and the three prismatic joints are active (i.e.,  $\theta_{0i}$  and  $d_i$ ,  $i = 1, \dots, 3$ ). The pivot joint angles,  $\theta_{i,i+3}$ , and the platform spherical joints,  $R_{i+3,E}$ , are passive.

The differential kinematics in the coordinate-free form is given by

$$\begin{aligned}
 \begin{bmatrix} \vec{\omega}_{0E} \\ \frac{d\vec{p}_{0E}}{dt^0} \end{bmatrix} &= \begin{bmatrix} \vec{z} & 0 & \vec{h}_1 & I \\ \vec{z} \times \vec{p}_{0E} & \vec{z} & \vec{h}_1 \times \vec{p}_{1E} & -\vec{p}_{4E} \times \end{bmatrix} \begin{bmatrix} \dot{\theta}_{01} \\ d_1 \\ \dot{\theta}_{14} \\ \vec{\omega}_{4E} \end{bmatrix} \\
 &= \begin{bmatrix} \vec{z} & 0 & \vec{h}_2 & I \\ \vec{z} \times \vec{p}_{0E} & \vec{z} & \vec{h}_2 \times \vec{p}_{2E} & -\vec{p}_{5E} \times \end{bmatrix} \begin{bmatrix} \dot{\theta}_{02} \\ d_2 \\ \dot{\theta}_{25} \\ \vec{\omega}_{5E} \end{bmatrix}
 \end{aligned}$$

$$= \begin{bmatrix} \vec{z} & 0 & \vec{h}_3 & I \\ \vec{z} \times \vec{p}_{0E} & \vec{z} & \vec{h}_3 \times \vec{p}_{3E} & -\vec{p}_{6E} \times \end{bmatrix} \begin{bmatrix} \dot{\theta}_{03} \\ \dot{d}_3 \\ \dot{\theta}_{36} \\ \vec{\omega}_{6E} \end{bmatrix}. \quad (9)$$

To reduce the complexity, we make the following change of variables (which is always possible for platform types of parallel mechanisms):

$$\vec{\omega}_{4E} = \vec{\omega}_{0E} - \vec{h}_1 \dot{\theta}_{14} \quad \vec{\omega}_{5E} = \vec{\omega}_{0E} - \vec{h}_2 \dot{\theta}_{25} \quad \vec{\omega}_{6E} = \vec{\omega}_{0E} - \vec{h}_3 \dot{\theta}_{36}. \quad (10)$$

To investigate unstable singularities, we lock all the active joints (i.e., set all the active joint rates to zero):

$$J_{C_p} \dot{\theta}_p = \begin{bmatrix} \vec{h}_1 \times \vec{p}_{14} & -\vec{h}_2 \times \vec{p}_{25} & 0 & \vec{p}_{54} \times \\ \vec{h}_1 \times \vec{p}_{14} & 0 & -\vec{h}_3 \times \vec{p}_{36} & \vec{p}_{64} \times \end{bmatrix} \begin{bmatrix} \dot{\theta}_{14} \\ \dot{\theta}_{25} \\ \dot{\theta}_{36} \\ \vec{\omega}_{0E} \end{bmatrix}. \quad (11)$$

Representing in a coordinate frame,  $J_{C_p}$  is a  $6 \times 6$  matrix. The mechanism is unstable if and only if that  $J_{C_p}$  loses rank. To simplify  $J_{C_p}$  further, we post-multiply  $J_{C_p}$  by a non-singular matrix ( $\vec{h}_n$  denotes the unit vector perpendicular to the platform):

$$J_{cp1} = J_{C_p} \begin{bmatrix} 1 & 0 & 0 & 0 & 0 & 0 \\ 0 & -1 & 0 & 0 & 0 & 0 \\ 0 & 0 & -1 & 0 & 0 & 0 \\ 0 & 0 & 0 & \vec{p}_{64} & \vec{p}_{54} & \vec{h}_n \end{bmatrix}.$$

Note that  $\begin{bmatrix} \vec{p}_{64} & \vec{p}_{54} & \vec{h}_n \end{bmatrix}$  is nonsingular, since  $\vec{p}_{64}$  and  $\vec{p}_{54}$  are always independent and  $\vec{h}_n$  is orthogonal to both of these vectors. After the multiplication and simplification using elementary column operations, we obtain

$$J_{cp1} = \begin{bmatrix} \vec{h}_1 \times \vec{p}_{14} & \vec{p}_{54} \times \vec{h}_n & \vec{h}_2 \times \vec{p}_{25} & \vec{h}_n & 0 & 0 \\ \vec{h}_1 \times \vec{p}_{14} & \vec{p}_{64} \times \vec{h}_n & 0 & \vec{0} & \vec{h}_3 \times \vec{p}_{36} & \vec{h}_n \end{bmatrix} \quad (12)$$

This matrix is singular if if any one of the following conditions hold:

1. Let  $\pi_1, \pi_2, \pi_3$ , as the planes that contain  $(\vec{h}_1, \vec{p}_{14}), (\vec{h}_2, \vec{p}_{25}), (\vec{h}_3, \vec{p}_{36})$ , respectively (i.e., the planes that contain the tangent vector to the base circle and the support arms). The mechanism is singular if any one of these planes,  $\pi_i$ , is coplanar with the platform. This is the same singularity that was found in [16] using numerical means. Specifically,

$$\vec{h}_1 \times \vec{p}_{14} \parallel \vec{h}_n \quad \text{or} \quad \vec{h}_2 \times \vec{p}_{25} \parallel \vec{h}_n \quad \text{or} \quad \vec{h}_3 \times \vec{p}_{36} \parallel \vec{h}_n. \quad (13)$$

2. There are also additional singularities that have not appeared in the literature. Define the following conditions:

$$(A1): \quad (\vec{h}_n \times (\vec{h}_n \times \vec{p}_{45})) \cdot (\vec{h}_1 \times \vec{p}_{14}) = 0$$

$$(A2): \quad (\vec{h}_n \times (\vec{h}_n \times \vec{p}_{45})) \cdot (\vec{h}_2 \times \vec{p}_{25}) = 0$$

$$(B1): \quad (\vec{h}_n \times (\vec{h}_n \times \vec{p}_{64})) \cdot (\vec{h}_1 \times \vec{p}_{14}) = 0$$

$$(B2): \quad (\vec{h}_n \times (\vec{h}_n \times \vec{p}_{64})) \cdot (\vec{h}_3 \times \vec{p}_{36}) = 0$$

$$(C1): \quad (\vec{h}_n \times (\vec{h}_n \times \vec{p}_{56})) \cdot (\vec{h}_3 \times \vec{p}_{36}) = 0$$

$$(C2): \quad (\vec{h}_n \times (\vec{h}_n \times \vec{p}_{56})) \cdot (\vec{h}_2 \times \vec{p}_{25}) = 0$$

The singular conditions then consist of any one of the two conditions in groups A, B, or C, and any one of the two conditions in the remaining two groups. Enumerating all combinations, we end up with 12 singularity conditions:

$$\{ (A1,B1), (A1,B2), (A1,C1), (A1,C2), (A2,B1), (A2,B2), (A2,C1), (A2,C2), (B1,C1), (B1,C2), (B2,C1), (B2,C2) \}.$$

To characterize these conditions geometrically, recall the definition of  $\pi_1, \pi_2, \pi_3$ , as the planes that contain  $(\vec{h}_1, \vec{p}_{14}), (\vec{h}_2, \vec{p}_{25}), (\vec{h}_3, \vec{p}_{36})$ , respectively. Then the singularity conditions above have the following interpretation:

$$\begin{aligned} (A1): & \quad \vec{p}_{45} \perp \pi_1 \\ (A2): & \quad \vec{p}_{45} \perp \pi_2 \\ (B1): & \quad \vec{p}_{64} \perp \pi_1 \\ (B2): & \quad \vec{p}_{64} \perp \pi_3 \\ (C1): & \quad \vec{p}_{56} \perp \pi_3 \\ (C2): & \quad \vec{p}_{56} \perp \pi_2. \end{aligned}$$

This means that, among the three sides of the triangle linking the spherical joints on the platform, if any two lie in the planes  $(\pi_1, \dots, \pi_3)$  that they are connected to (there are two possibilities each), the mechanism is singular. A particular case is as shown in Figure 3 where the platform face is vertical which may occur during turning type of operation.

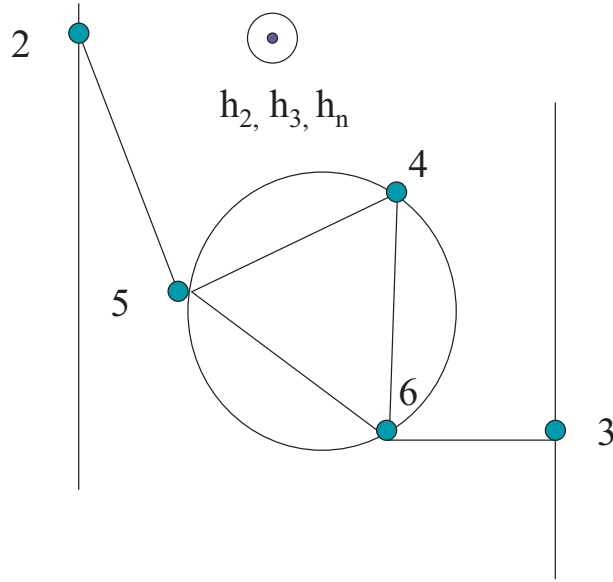


Figure 3: Example of Eclipse Singularity

We will also use a planar platform to illustrate the coordinate-independent approach to finding unstable singularities. Consider a planar platform mechanism as shown in Figure 4. After eliminating the joint velocity  $\dot{\theta}_4, \dots, \dot{\theta}_6$  as in (10) and locking the active prismatic joints of the legs, the constraint Jacobian can be written as

$$J_{C_p} \theta_p = \begin{bmatrix} \vec{z} \times \vec{p}_{14} & -\vec{z} \times \vec{p}_{25} & 0 & \vec{z} \times \vec{p}_{45} \\ \vec{z} \times \vec{p}_{14} & 0 & -\vec{z} \times \vec{p}_{36} & \vec{z} \times \vec{p}_{46} \end{bmatrix} \begin{bmatrix} \dot{\theta}_1 \\ \dot{\theta}_2 \\ \dot{\theta}_3 \\ \dot{\theta}_E \end{bmatrix}. \quad (14)$$

The singular configurations are given by (see Figure 5):

$$(A): \quad \vec{p}_{14} \parallel \vec{p}_{25} \parallel \vec{p}_{36}$$

- (B):  $\vec{p}_{14} \parallel \vec{p}_{25} \parallel \vec{p}_{45}$   
(C):  $\vec{p}_{25} \parallel \vec{p}_{36} \parallel \vec{p}_{45}$   
(D):  $\vec{p}_{14} \parallel \vec{p}_{36} \parallel \vec{p}_{45}$ .  
(E):  $\vec{p}_{14} \parallel \vec{p}_{4I}$  and  $\vec{p}_{25} \parallel \vec{p}_{5I}$   
where  $I$  is any point along  $\vec{p}_{36}$

Singularity (A) corresponds to all three legs parallel. Singularities (B)-(D) correspond to any two of the legs collinear with the platform. Singularity (E) corresponds to all three legs intersecting at the point  $I$ . It is easy to see that  $J_{C_p}$  loses rank for singularities (A)-(D). To see Case (E), the following elementary column operations are helpful:

$$\begin{aligned}
J_{C_p} &= \begin{bmatrix} \vec{z} \times \vec{p}_{14} & -\vec{z} \times \vec{p}_{25} & 0 & \vec{z} \times \vec{p}_{45} \\ \vec{z} \times \vec{p}_{14} & 0 & -\vec{z} \times \vec{p}_{36} & \vec{z} \times \vec{p}_{46} \end{bmatrix} \\
&\sim \begin{bmatrix} \vec{z} \times \vec{p}_{14} & -\vec{z} \times \vec{p}_{25} & 0 & \vec{z} \times \vec{p}_{4I} - \vec{z} \times \vec{p}_{5I} \\ \vec{z} \times \vec{p}_{14} & 0 & -\vec{z} \times \vec{p}_{36} & \vec{z} \times \vec{p}_{4I} - \vec{z} \times \vec{p}_{6I} \end{bmatrix} \\
&\sim \begin{bmatrix} \vec{z} \times \vec{p}_{14} & -\vec{z} \times \vec{p}_{25} & 0 & \vec{z} \times \vec{p}_{4I} - \vec{z} \times \vec{p}_{5I} \\ \vec{z} \times \vec{p}_{14} & 0 & -\vec{z} \times \vec{p}_{36} & \vec{z} \times \vec{p}_{4I} \end{bmatrix} \\
&\quad (\text{since } \vec{p}_{6I} \text{ is collinear with } \vec{p}_{36}).
\end{aligned}$$

Though the coordinate-free form of  $J_{C_p}$  facilitates finding geometric conditions for the unstable singularities, it is difficult to state in general if *all* the singularities are found. In the case of the planar platform, through a careful analysis of the null space of  $J_{C_p}$  for all possible cases, we can in fact conclude that the above are all possible singularities.

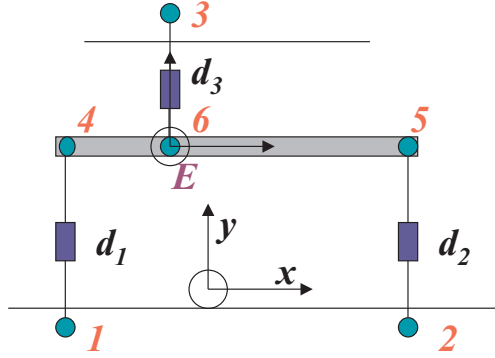


Figure 4: Planar Platform Mechanism

### 3 Methods for Arresting Kinematic Instability

Kinematic instability is a direct consequence of passivity in the parallel mechanism. At certain poses, the active joints cannot resist task wrenches in certain directions, and end-effector self motion is possible due to passive joint self motion. It is intuitive that solutions to this problem involve either redundancy or application of additional constraint.

#### 3.1 Redundant Actuation

As an example, we again consider a planar Stewart Platform shown in 6. The pose of the mechanism in figure 6 is unstable. Forces applied to the end-effector in a direction orthogonal to the actuators cannot be resisted by the mechanism.

A possible remedy for this is to introduce a new set of active joint space variables in the form of an additional active kinematic chain. An example of this is shown in figure 7, where a 2R planar “finger” grasps

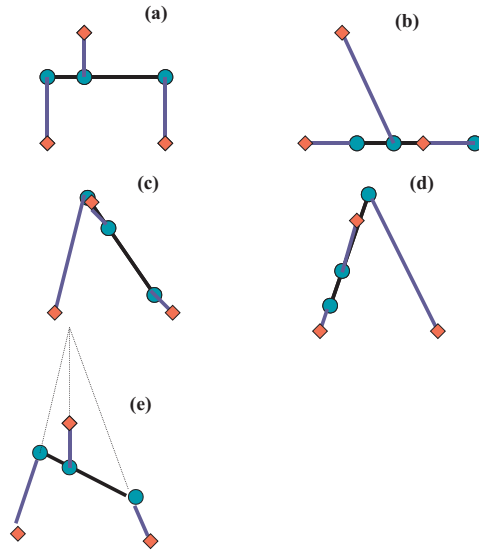


Figure 5: Singular Configurations of Planar Platform Mechanism

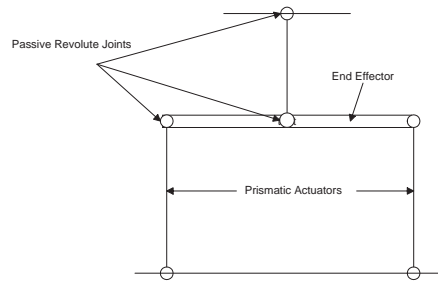


Figure 6: Planar Stewart Platform in Unstable Pose

the Stewart Platform at a passive joint. The resulting mechanism is a closed kinematic system with four chains, and is stable in a kinematic sense.

While the new mechanism is stable, this approach has several problems. The cost of the complete mechanism is considerably increased as new actuator and sensor hardware is required. The support “finger” needs to find the grasp point on the Stewart Platform (note that this point can be anywhere on the mechanism), and link up appropriately. This may require complex reference sensing, and an intricate end-effector gripper for the support mechanism. With the support finger attached to the platform, the mechanism is redundantly actuated, as five joint-space DOFs map to three task space DOFs. It is suggested that the intermittent need for this support may not warrant its complexity.

Another approach involving redundant actuation activates an existing passive joint in the mechanism. Figure 8 is an example using the Stewart Platform where one of the base revolute joints is activated. The mechanism is has one redundant degree of freedom, and is stable. While this method does not have the complexity of mating mechanisms, it may also not be feasible to replace a passive joint with actuator hardware and sensing.

### 3.2 Additional Constraint

Another method to eliminate unstable singularity is to apply additional constraint to the mechanism. In past literature, this has taken the form of bracing, where contact with a fixed surface or passive mechanism

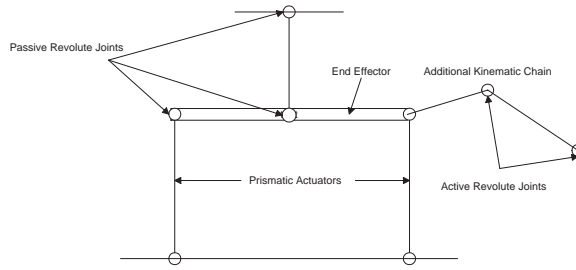


Figure 7: Planar Stewart Platform with Additional Active Kinematic Chain

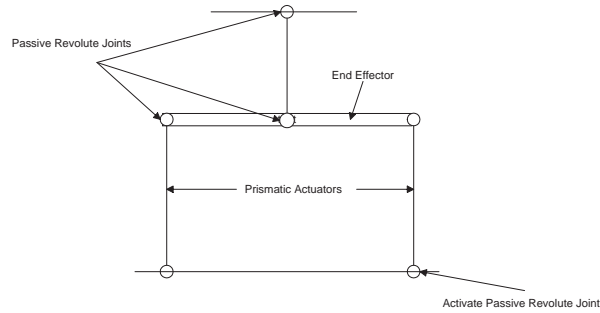


Figure 8: Planar Stewart Platform with Activated Passive Joint

constrains the robot from motion in selected task directions. A classic example of bracing is the application of the bridge to the pool cue. In a planar context, the pool cue grasped in one hand is manipulable in 3 DOF. However, the task requires little or no motion off the cue axis. The bridge applies constraint to the cue to disallow this motion. While this is not an example of unstable singularity as the manipulator is serial, the application reduces manipulability, which can be a key trade-off in kinematically stabilizing a parallel robot.

Figure 9 shows the planar Stewart Platform with an external brace. The contact between the platform and the brace is such that no motion parallel to the end-effector is possible, thus the mechanism is stable. This is another illustration of the trade-off between manipulability and stability. The method of external bracing has many of the same complications as redundant actuation using a second active finger, including the task where the Stewart Platform “finds” the external brace, and the required grasp is made. Referring again to the pool cue example, the mating of the cue to the bracing hand or bridge requires stereo vision (eyes), and tactile sensing (skin). While this action is taken somewhat for granted by humans, it can be an involved task for robots. The complications seem somewhat expensive in the kinematic stabilization role

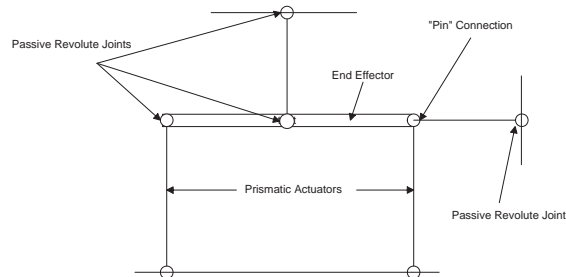


Figure 9: Planar Stewart Platform with External Brace

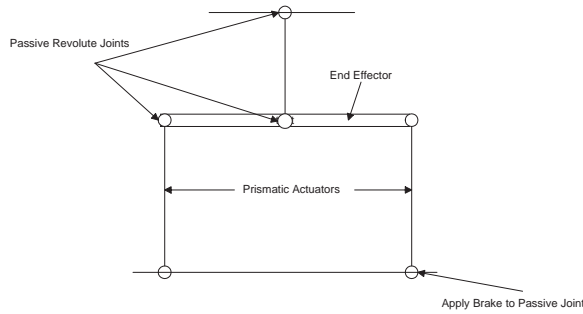


Figure 10: Planar Stewart Platform with Braked Passive Joint

considering the the constraint delivered is required only in a small subset of the robot’s workspace.

Analogous to activation of a passive joint is applying constraint using a passive joint, illustrated on the Stewart Platform in figure 10. This method applies a brake to the passive joint when the mechanism is in the close neighborhood of unstable singularity. The trade-off is that the mechanism is unmanipulable in the locked condition. As the brake is embedded in the mechanism, there is no requirement of an external mechanism, and the cost and significant complexity of this is eliminated. The passive joint brake may provide a less expensive and efficient alternative to redundant actuation.

## 4 Conclusions

Parallel mechanism offers advantages such as superior load to weight ratio and stiffness. However, finding and avoiding unstable configurations in the workspace is in general a difficult task. Singularity determination is usually done through an exhaustive search of the workspace. This procedure is time consuming, may miss some singularities due to the granularity of the search, and does not offer ready geometric insight of these configurations. In this paper, we present a coordinate-free approach to finding the unstable singularities. We illustrated the procedure using a 6-DOF parallel machining center and a 3-DOF planar platform. Though we cannot yet claim to have located *all* of the singularities, this procedure has already produced singularities that have not been previous found.

We have also discussed different strategies in dealing with the unstable singularities during manipulation, including redundant actuation, additional constraint, and active braking.

Current research focuses on determining necessary and sufficient conditions for unstable singularities using the coordinate-free form of the constraint Jacobian, and stability condition for motion control with active braking.

## Acknowledgment

This work is supported in part by the Center for Advanced Technology in Automation, Robotics & Manufacturing under a block grant from the New York State Science and Technology Foundation, the National Science Foundation (Grant IIS-9820709), and a U.S. Department of Energy Integrated Manufacturing Predoctoral Fellowship.

## References

- [1] M. Husty and A. Karger, “Self-motions of griffis-duffy type parallel manipulators,” *IEEE International Conference of Robotics and Automation*, San Francisco, CA, 2000.
- [2] M. Husty and A. Karger, “On self-motions of a class of parallel manipulators,” in *Advances in Robot Kinematics*, Kluwer Academy Publishing, pp. 439-449, 1996.
- [3] A. Karger and M. Husty, “Recent results of self motions of parallel mechanisms,” *Proceedings of RAAD*, 1997.

- [4] G. Dordevic, M. Rasic, D. Kostic and D. Surdilovic, "Learning of inverse kinematics behavior of redundant robots," *IEEE International Conference on Robotics and Automation*, Detroit, MI, 1999.
- [5] J.-P. Merlet, "Parallel manipulators: state of the art and perspective," in *Robotics, Mechatronics and Manufacturing Systems*, Elsevier, 1993.
- [6] J.P. Merlet, "Parallel manipulators 2: The theory, singular configurations and Grassman geometry," *Technical Report No. 791*, INRIA, France, 1988.
- [7] J.P. Merlet, "Singular configurations of parallel manipulators and Grassman geometry," *International Journal of Robotics Research*, Vol,8, No. 5, pp. 45-56, 1989.
- [8] A. Bicchi, C. Melchiorri, and D. Balluchi, "On the mobility and manipulability of general multiple limb robots," *IEEE Transactions on Robotics and Automation*, pp. 215-228, April 1995.
- [9] P. Chiacchio, S. Chiaverini, L. Sciavicco, and B. Siciliano, "Global task space manipulability ellipsoids for multiple-arm systems," *IEEE Transactions of Robotics and Automation*, vol. 7, pp. 678-685, October 1991.
- [10] F. Park and J. Kim, "Manipulability and singularity analysis of multiple robotic systems: A geometric approach," in *Proc. 1998 International Conference on Robotics and Automation* (Leuven, Belgium), pp. 1032-1037, May 1998.
- [11] A. Bicchi and D. Prattichizzo, "Manipulability of cooperating robots with passive joints," in *Proc. 1998 IEEE International Conference on Robotics and Automation*, (Leuven, Belgium), pp. 1038-1044, May 1998.
- [12] A. Bicchi and D. Prattichizzo, "Manipulability of cooperating robots with unactuated joints and closed-chain mechanisms," *IEEE Transactions on Robotics and Automation*, Vol.16, No.4, August 2000.
- [13] A. Bicchi, "On the closure properties of robotic grasping," *Int. J. Robot Res.*, vol.14, no.4, pp.319-334, 1995.
- [14] J. Wen and L. Wilfinger, "Kinematic manipulability of general constrained rigid multibody systems," in *Proc. 1998 IEEE International Conference on Robotics and Automation*, (Leuven, Belgium), pp. 1020-1025, May 1998.
- [15] C. Gosselin and J. Angeles, "Singularity analysis of closed-loop kinematic chains," *IEEE Transactions on Robotics and Automation*, Vol. 6, and No. 3, June 1990.
- [16] S.J. Ryu, C. Park, J. Kim, J. Hwang, J. Kim, F.C. Park, "Design and performance of a parallel mechanism-based universal machining center,"
- [17] J. Kim, F.C. Park, S. Ryu, J. Kim, J. Hwang, C. Park, and C. Iurascu, "Design and analysis of a redundantly actuated parallel mechanism for rapid machining,"
- [18] J. Kim, F.C. Park, J. Lee, "A new parallel mechanism machine tool capable of five-face machining,"
- [19] S. Lee, "Dual redundant arm configuration optimization with task-oriented dual arm manipulability," *IEEE Transactions on Robotics and Automation*, Vol. 3, No. 1, February 1989.
- [20] Z. Li, P. Hsu, and S. Sastry, "Grasping and coordinated manipulation by a multifingered robot hand," *International Journal of Robotics Research*, Vol. 8 No. 4, August 1989.
- [21] K. Zanganeh and J. Angeles, "Kinematic isotropy and design of parallel manipulators," *International Journal of Robotics Research*, Vol. 16, No. 2, April 1997.
- [22] T. Kokkinis and B. Paden, "Kinetostatic performance limits of cooperating manipulators using force-velocity polytopes," in *Proceedings ASME Winter Annual Meeting*, November 1989.

- [23] J.L. Olazagoitia, and A. Avello, "Application of global optimization techniques to the practical construction of stewart platforms,"
- [24] L. Stocco, S.E. Salcudean, and F. Sassani, "Matrix normalization for optimal robot design," *Proceedings 1998 IEEE International Conference on Robotics and Automation*, , May 1998.
- [25] S. Leguay-Durand and C. Reboulet, "Optimal design of a redundant spherical parallel manipulator," *Robotica* Vol. 15 1997.
- [26] F. Hao and J.M. McCarthy, "Conditions for line-based singularities in spatial platform manipulators," *Journal of Robotic Systems*, pp.43-55, 1998.
- [27] J. O'Brien and J. Wen, "Redundant actuation for improving kinematic manipulability," *IEEE International Conference on Robotics and Automation*, Detroit, MI, May 1999.
- [28] S. Chiaverini, B. Siciliano, and O. Egeland, "Review of the damped least squares inverse kinematics with experiments on an industrial robot manipulator," *IEEE Transactions on Control Systems Technology*, Volume 2, Number 2 pp. 123, June 1994.
- [29] J. Craig, *Introduction to Robotics* , Addison-Wesley, New York, 1989.